

# Nanoparticle-Mediated Gene Transfer From Electrophoretically Coated Metal Surfaces

Anna Kovtun,<sup>†</sup> Sebastian Neumann,<sup>‡</sup> Manuel Neumeier,<sup>†</sup> Henning Urch,<sup>†</sup> Rolf Heumann,<sup>‡</sup> Michael M. Gepp,<sup>§</sup> Katrin Wallat,<sup>†</sup> Manfred Koeller,<sup>¶</sup> Heiko Zimmermann,<sup>§</sup> and Matthias Epple\*,<sup>†</sup>

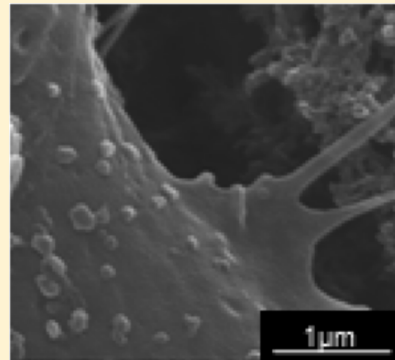
<sup>†</sup>Inorganic Chemistry and Center for Nanointegration Duisburg-Essen (CeNIDE), University of Duisburg-Essen, 45117 Essen, Germany

<sup>‡</sup>Chair of Biochemistry, Faculty of Chemistry and Biochemistry, University of Bochum, Universitaetsstrasse 150, 44780 Bochum, Germany

<sup>§</sup>Fraunhofer Institute for Biomedical Engineering (IBMT) and Chair for Molecular and Cellular Biotechnology, University of Saarbruecken, Ensheimer Strasse 48, 66386 St. Ingbert, Germany

<sup>¶</sup>Bergmannsheil University Hospital/Surgical Research, Ruhr-University of Bochum, 44789 Bochum, Germany

**ABSTRACT:** The transfer of genetic information into living cells is a powerful tool to manipulate their protein expression by the regulation of protein synthesis. This can be used for the treatment of genetically caused diseases (gene therapy). However, the systemic application of genes is associated with a number of problems, such as a targeted gene delivery and potential side effects. Here we present a method for the spatial application of nanoparticle-based gene therapy. Titanium was electrophoretically coated with DNA-functionalized calcium phosphate nanoparticles. NIH3T3 cells and HeLa cells were transfected with pcDNA3-EGFP. We monitored the transfection *in vitro* by fluorescence microscopy, flow cytometry, and Western Blot analysis. By coating a transparent substrate, i.e., indium tin oxide (ITO), with nanoparticles, we followed the transfection by live cell imaging.



## 1. INTRODUCTION

The transfer of genetic information into living cells to manipulate their protein expression pattern is of high interest in cell biology and in the treatment of genetically caused diseases. The latter is called “gene therapy” and constitutes an expanding area of current biomedical research.<sup>1</sup> In principle, the production of specific proteins by a cell can be triggered by introducing the corresponding plasmid DNA into the cell nucleus where it is then transcribed into messenger RNA (mRNA), which is finally translated into the corresponding protein in the cytosol (“transfection”).<sup>2–4</sup> On the other hand, the production of proteins within a cell can be specifically turned off by the introduction of small interfering RNA (siRNA) into the cytoplasm (“gene silencing”).<sup>5–7</sup> Due to the fact that nucleic acids alone are not able to enter a cell, suitable carriers are needed. Besides physical methods such as electroporation and the gene gun, viral carriers and nanoparticulate carriers are often used.<sup>8</sup> However, considering general concerns about viral transfection agents for clinical application,<sup>9</sup> other systems such as cationic organic transfection agents<sup>10</sup> and inorganic nanoparticles<sup>8</sup> are prominent nonviral carriers.

In general, all these delivery systems are available in dispersed form, which has to be administered into the desired tissue or must be given systemically. Even if a given system has high transfection efficiency, there remains the question of the

local application where the action is desired. Clinically, this may be the environment of an implant where a stimulating action by cell-specific protein synthesis is desired. An example that immediately comes into mind is an endoprosthesis (hip, knee, tooth), where a fast and stable attachment of bone is desired. This may be enhanced by the induction of the synthesis of bone growth-stimulating factors (e.g., bone morphogenetic proteins (BMPs)) or vascularizing proteins (e.g., vascular endothelial growth factor (VEGF)). Another application may be the induction of spinal fusion.<sup>11</sup> There are only few approaches reported about a spatially directed and efficient delivery of nucleic acids. These include multilayer polyelectrolyte/nucleic acid coatings,<sup>12,13</sup> DNA encapsulated into biodegradable polymers,<sup>14</sup> the attachment of DNA on anti-DNA antibodies that are themselves covalently attached to an implant surface,<sup>15,16</sup> and the incorporation of polymeric DNA-nanocarriers into calcium phosphate cement<sup>17</sup> or hydrogels.<sup>18</sup> An *in vitro* bone formation by an adenovirus encoding BMP-13 was reported by Helm et al.<sup>11</sup> Surface-mediated delivery systems that contain DNA embedded into polyelectrolyte layers make use of poly(ethyleneimine) and poly(allylamine)

**Special Issue:** Electrophoretic Deposition

**Received:** April 10, 2012

**Revised:** June 27, 2012

**Published:** June 29, 2012

hydrochloride)<sup>19</sup> poly-L-lysine,<sup>20</sup> poly(2-aminoethyl propylene phosphate),<sup>21</sup> and poly(L-tartaramido pentaethylene tetraamine)<sup>22</sup> as cationic polyelectrolytes. DNA can also be encapsulated into porous PLGA scaffolds, leading to a good efficiency *in vivo*.<sup>23</sup> A limitation of all these techniques is the application of large amounts of synthetic polymers with sometimes unknown biological action.

A nanoparticle-mediated gene transfer from a metal surface has not been reported so far. Inorganic nanoparticles for transfection consisting of gold, silica, or carbon nanotubes are well-known.<sup>8,24</sup> In addition, organic nanoparticulate carriers such as liposomes or polymers are well established.<sup>3,10,25</sup> However, some inorganic nanoparticles are not biodegradable (such as gold or carbon nanotubes), and “soft” polymeric nanoparticles and liposomes cannot be easily assembled on a solid surface. In the latter case, a layer-by-layer system would be better suited. If a biocompatible inorganic nanoparticle system such as calcium phosphate (CaP) was used, such a system would be ideally suited to create a bioactive surface in bone contact, taking into account that the inorganic phase of bone consists of calcium phosphate nanoparticles.<sup>26–29</sup> Based on our previous experience with poly(ethylenimine)-stabilized nucleic acid-functionalized calcium phosphate nanoparticles (CaP/PEI/DNA) for transfection,<sup>30–32</sup> gene silencing,<sup>33</sup> and drug delivery into cells,<sup>34</sup> we here report on a straightforward method to coat metallic surfaces with calcium phosphate nanoparticles by electrophoresis,<sup>35–37</sup> forming a coating that is both osteoconductive and bioactive.

## 2. MATERIALS AND METHODS

**2.1. Electrophoretic Coating of Conducting Surfaces with CaP/PEI/DNA Nanoparticles.** As substrate, titanium plates or ITO-glass plates (indium tin oxide-coated glass; electrically conducting and transparent) with a size of 10·10 mm<sup>2</sup> were used. For the bioactive coating, the CaP/PEI nanoparticles were produced as follows:<sup>38</sup> Aqueous solutions of Ca(NO<sub>3</sub>)<sub>2</sub>·4 H<sub>2</sub>O (19.91 mM, Riedel-de Haen, Seelze, Germany) and (NH<sub>4</sub>)<sub>2</sub>HPO<sub>4</sub> (11.94 mM, Aldrich, Steinheim, Germany) were adjusted to pH 9 with 1.0 M NaOH and then rapidly mixed with a peristaltic pump with a speed of 1.35 mL min<sup>-1</sup>. Simultaneously, the PEI solution (2 g L<sup>-1</sup>; Aldrich, Steinheim, Germany) was added to the calcium phosphate solution with a rate of 2.6 mL min<sup>-1</sup>. Then the nanoparticles were filtered through a 100 nm filter (Pall Life Sciences) and dried at room temperature.

For the electrophoretic coating of the plates, the nanoparticles were resuspended in 2-propanol (15.4 mg mL<sup>-1</sup>) by 30 min incubation in an ultrasonic bath. Then, pcDNA3-EGFP solution in endotoxin-free water (purified from *Escherichia coli* using the Qiagen Plasmid Maxi kit, Qiagen, Hilden, Germany) was added to achieve a final DNA concentration of 100 µg mL<sup>-1</sup>. The plates were coated with a voltage of 50 V for 30 s, as described in ref 39. To estimate the layer thickness and the amount of deposited nanoparticles, the calcium content was determined by atomic absorption spectroscopy (AAS). Both substrates were coated with CaP/PEI/DNA nanoparticles and, as control samples, also with CaP/PEI nanoparticles.

**2.2. Transfection from electrophoretically coated metal surfaces.** For the transfection experiments, NIH3T3 cells (a mouse embryonic fibroblast cell line) and HeLa cells (a human epithelial carcinoma cell line) were used. NIH3T3 cells were cultivated in RPMI 1640 (PAA Laboratories GmbH, Cölbe, Germany) supplemented with 10% fetal calf serum

(FCS), 2 mM glutamine, 100 U mL<sup>-1</sup> penicillin, and 100 U mL<sup>-1</sup> streptomycin, whereas HeLa cells were cultivated in Dulbecco's modified Eagle's medium (DMEM; Gibco, Life Technologies GmbH, Darmstadt, Germany) supplemented with 10% fetal bovine serum (FBS), 100 U mL<sup>-1</sup> penicillin, and 100 U mL<sup>-1</sup> streptomycin at 37 °C in humidified atmosphere with 5% CO<sub>2</sub> (NIH3T3) or 10% CO<sub>2</sub> (HeLa).

5 × 10<sup>4</sup> cells were seeded per well in the 24-well plate onto the plates with one plate of 10 × 10 mm<sup>2</sup> in each well. The duration of the transfection by cultivation on the wells was 7 h. Afterward, the transfection medium was replaced with fresh cell culture medium. The efficiency of the transfection was measured after approximately 48 h of cell incubation by fluorescence microscopy, flow cytometry, and Western Blot analysis. For these analyses, the plates were relocated into fresh 24-well plates (to remove the cells that had grown on the plastic well and not on the plates) and washed twice with PBS.

**2.2.1. Transfection from Conducting Surfaces Coated with CaP/PEI/DNA Nanoparticles.** The plates coated with CaP/PEI/DNA nanoparticles were placed into the 24-well plates. Then the cells were seeded onto the plates and 500 µL of the corresponding cell culture medium was added. After 7 h, the cell culture medium was replaced with fresh medium.

**2.2.2. Transfection from Conducting Surfaces Coated with CaP/PEI Nanoparticles Followed by Addition of DNA by Dripping.** The plates coated with CaP/PEI nanoparticles were placed into the 24-well plate. Then 4 µL of DNA solution (1 mg mL<sup>-1</sup>) was dripped onto the surface and dried at 37 °C. Afterward, the cells were seeded on the plates, and 500 µL of the cell culture medium was added. After 7 h, the cell culture medium was replaced by fresh medium. The amount of DNA was 4 µg cm<sup>-2</sup>.

**2.2.3. Control Experiments.** As a control we used non-transfected cells and cells transfected with Polyfect from solution (according to the protocol described in ref 40), both seeded on the uncoated conducting surface (titanium or ITO glass). As a further control, plates coated with CaP/PEI nanoparticles only (i.e., no DNA at all) were seeded with cells. Then 500 µL of the cell culture medium was added, and the cells were treated as described in Section 2.2.

**2.3. Cell Fixation and Scanning Electron Microscopy (SEM).** The cells were cultivated on the plates for 48 h, then fixed with 3% glutaraldehyde, dehydrated in an ascending ethanol row (20, 40, 60, 80 and 96%), and finally subjected to critical point drying. SEM was performed with a FEI Quanta 400 ESEM instrument in high vacuum. Sputtering was performed with gold–palladium for 1.5 min.

**2.4. Microscopy.** The transfection efficiency was determined using transmission light microscopy and fluorescence microscopy with a Zeiss Axiovert 40 CFL microscope (Carl Zeiss MicroImaging GmbH, Cologne, Germany). For live-cell imaging, a BioStation IM Live Cell Recorder (Nikon GmbH, Duesseldorf, Germany) was used.

**2.5. Flow cytometry of NIH3T3 cells.** Flow cytometry was performed on a FACSCalibur instrument and on a CyFlow SL instrument. The data were analyzed with the WinMDI 2.9 software. For flow cytometry, the cells were trypsinized, transferred into Eppendorf tubes, washed with cell culture medium with supplements as described in Section 2.2, fixed with 100 µL 3% paraformaldehyde (Janssen Chimika, Belgium), washed twice with PBS, and then resuspended in PBS.

**2.5. Western Blot Analysis.** Cells were lysed in ice-cold 2× lysis buffer (100 mM Tris-HCl pH 7.4, 300 mM NaCl, 2% (w/v) NP-40, 80 mM NaF, 20 mM EDTA, 0.2% (w/v) sodium dodecyl sulfate (SDS), 2 mM sodium orthovanadate, 0.2% (w/v) sodium desoxycholate, 30 mM MgCl<sub>2</sub>, 2× Roche Protease Inhibitor). The lysates were centrifuged (13 000g, 5 min, 4 °C), and the protein concentration in the supernatants was determined with the DC protein assay (Bio-Rad Laboratories, Hercules, CA, USA). Equal amounts of protein were resolved by 12% polyacrylamide gels (Table 1). The proteins were

**Table 1. The Composition of the SDS-PAGE Gel for Protein Separation**

	separation gel (12%)	stacking gel (4%)
30% acrylamide solution	4.0 mL	410 μL
water	3.4 mL	1.8 mL
lower Tris pH 8.8	2.5 mL	
upper Tris pH 6.8		750 μL
10% APS	100 μL	60 μL
TEMED	5 μL	3 μL

blotted to 0.2 μm nitrocellulose (Schleicher & Schuell, Dassel, Germany) and blocked by 1 h incubation in 5% powdered milk dissolved in TBS-T (10 mM Tris-HCl, pH 7.6, 150 mM NaCl, 0.05% Tween 20) at ambient temperature. EGFP-expression was detected using an anti-EGFP antibody (dilution 1:1000 in TBS-T, abcam, Cambridge, UK) followed by a horseradish peroxidase-conjugated secondary antibody (dilution 1:3000 in TBS-T, Dianova, Hamburg, Germany) and finally by the enhanced chemiluminescence substrate detection kit (Super-Signal West Pico Chemiluminescent Substrate, Thermo Fisher Scientific Inc., Rockford, IL USA).

**2.6. Statistics.** Errors are given as standard deviations. *P*-values were calculated using Student's *t* test. *P*-values > 0.05 were considered as insignificant.

### 3. RESULTS AND DISCUSSION

Bioactive surfaces were prepared by electrophoretic coating of titanium or ITO with calcium phosphate nanoparticles. The electrophoretic deposition of calcium phosphate (nano)-particles to improve the bioactivity of implant surfaces is well accepted today.<sup>35–37,41</sup> We prepared calcium phosphate nanoparticles functionalized with PEI by precipitation. Dynamic light scattering of the particles gave a size of the CaP/PEI nanoparticles of 149 nm and a ζ potential of +38 mV.<sup>38</sup> Electrophoretic coating was carried out at a voltage of 50 V for 30 s, leading to a smooth coating on the titanium surfaces. By AAS, we determined the amount of calcium in a deposited layer after dissolution in 1 M HCl to 25 μg cm<sup>-2</sup>. This corresponds to 63 μg hydroxyapatite cm<sup>-2</sup>. With a density of hydroxyapatite of 3160 kg m<sup>-3</sup>, the thickness of the layer is about 200 nm. If we assume a close packing of spheres of equal size with a packing density of 74%, the effective layer thickness is computed with 200/0.74 = 270 nm. If we now assume an average particle diameter of 100 nm, the coating consists of about three layers of nanoparticles. Note that this is just an approximation with a probable error of at least 10% because the packing density is not really known and can only be estimated. A schematic setup of the electrophoresis apparatus and scanning electron micrographs of the particles deposited on the titanium surface are shown in Figure 1. The coating gives a thin and smooth layer of nanoparticles on the metal surface.

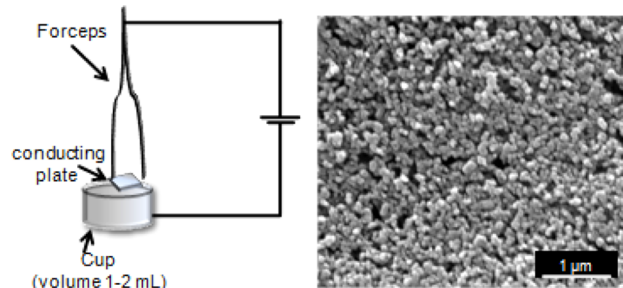


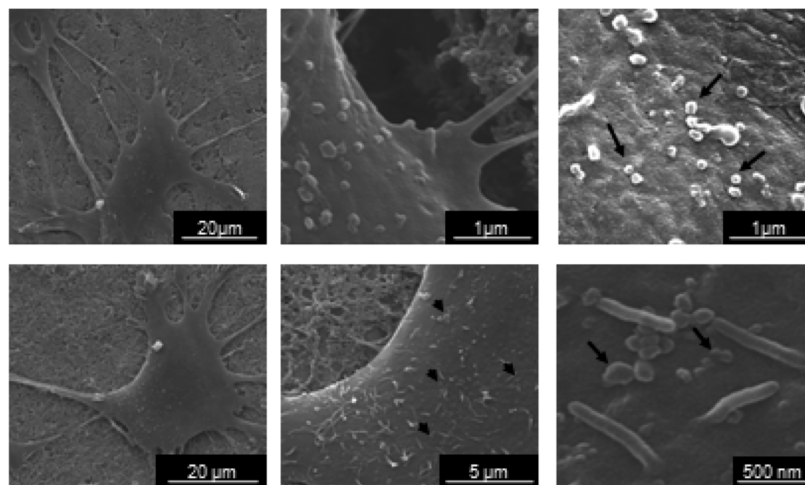
**Figure 1.** Schematic setup of the electrophoresis apparatus (left) and a representative electron micrograph of a CaP/PEI nanoparticle-coated titanium surface (right).

We analyzed the cytocompatibility of the coatings and the attachment of cells to the surface by SEM. A morphological analysis of the cell culture by SEM showed an excellent adhesion of the cells to the substrate and also a large number of nanoparticles on the cell surface (Figure 2). The nanoparticles were also found on the upper surface of the cells, presumably due to the special method of cell locomotion on the coating. Such a tight contact of the cell membrane with a large number of particles probably enhances the chance of the nanoparticles to be taken up via endocytosis. The situation is different compared to the standard methods of transfection where the dispersed nanoparticles are used, which only rarely meet the cell surface. Also, the spreading of the cells on the coating and their good adhesion indicated that cells remained healthy.

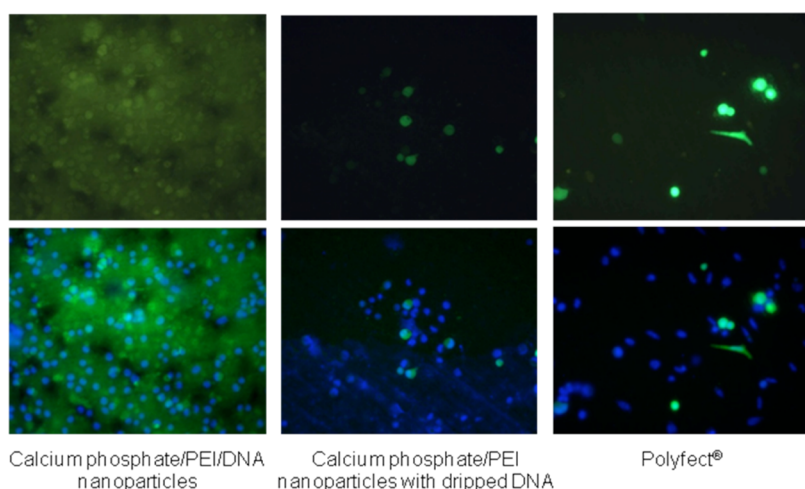
The transfection efficiency was measured by fluorescence microscopy, flow cytometry, and Western blot analysis. The cell nuclei were additionally stained with 4',6-diamidino-2-phenylindole (DAPI) to determine the total number of cells on the substrate in comparison to the green fluorescing cells. The results of reflected-light fluorescence microscopy are shown in Figure 3.

Figure 3 shows the total number of cells on the plate (DAPI; blue) and the successfully transfected cells (EGFP; green). However, due to the autofluorescence of the cells and a background fluorescence of the coating itself (especially well visible in Figure 3, left), the numerical determination of the transfection efficiency by counting fluorescing cells was difficult. Therefore, we performed flow cytometry of the samples (Table 2).

NIH3T3 cells seeded on titanium substrate were used as a standard for the living population and as a negative control for the EGFP transfection efficiency. The living population was defined and gated according to the FSC/SSC parameters (Forward Scatter or FSC, i.e., a detector in line with the light beam, and Side Scatter or SSC, i.e., a detector perpendicular to the light beam) individually for each set of experiments. The region with living cells was analyzed by dot plot analysis using two parameters: FSC and EGFP fluorescence intensity. The square statistics were used to analyze single-positive (only on one axis) and double-positive (on both axes) cells. Live cells were selected according to their granularity, gated in the left upper square, and were assumed to be EGFP-negative. The gate for EGFP was set according to this population, and all samples were analyzed accordingly to these square statistics. The background in the negative control (NIH3T3 cells seeded on titanium substrate) was 2.4%. Presumably, these were dust particles or impurities in dispersion. The cells transfected with Polyfect showed a transfection efficiency of about 17%, and



**Figure 2.** Scanning electron micrograph of NIH3T3 fibroblasts grown on a CaP/PEI/DNA nanoparticle-coated titanium surface. Top row: Cells seeded on the CaP/PEI/DNA nanoparticle coating; bottom row: Cells seeded on the CaP/PEI nanoparticle coating with dripped DNA. Black arrows indicate nanoparticles on the cell surface.



**Figure 3.** Fluorescence microscopy of NIH3T3 cells seeded on a CaP/PEI/DNA nanoparticle-coated titanium surface (left), cells seeded on a CaP/PEI nanoparticle-coated titanium plate with dripped DNA (center), and cells transfected from dispersion with Polyfect on a titanium substrate (right). Transfected cells are green due to the expression of EGFP. Top row: Cells expressing EGFP; bottom row: Overlay images of cells expressing EGFP with DAPI staining (blue; magnification: 200 $\times$  in all cases).

**Table 2. Efficiency of EGFP-Gene Transfer to NIH3T3 Cells as Determined by Flow Cytometry ( $N = 3$ )<sup>a</sup>**

sample	efficiency $\pm$ SD/%
control cells on titanium	2.4 $\pm$ 0.3
cells on CaP/PEI/DNA-nanoparticle coating on titanium	14 $\pm$ 5 ( $P < 0.05$ )
cells on CaP/PEI-nanoparticle coating on titanium with dripped DNA	16 $\pm$ 9 ( $P < 0.01$ )
cells on CaP/PEI nanoparticle coating on titanium without DNA	6 $\pm$ 3
cells on titanium, treated with Polyfect in dispersion	17 $\pm$ 12

<sup>a</sup>P-values are given in comparison to cells cultured on a CaP/PEI-coating without DNA.

cells seeded on titanium substrate coated with CaP/PEI/DNA and CaP/PEI nanoparticles with dripped DNA showed a comparable transfection efficiency. The observed 6% in the negative control (cells grown on CaP/PEI coating without DNA) may result from particles that have detached from the coating and showed a weak autofluorescence at this wavelength. This can be also observed in Figure 3 (left).

To confirm the expression of EGFP and to exclude cellular autofluorescence, we additionally performed Western blot analysis of all samples. The results are shown in Figure 4.



**Figure 4.** Western Blot of NIH3T3 cells after transfection with different techniques. (A) Cells on a CaP/PEI nanoparticle coating with dripped DNA; (B) cells on a CaP/PEI/DNA nanoparticle coating; (C) cells on titanium, treated with Polyfect in dispersion; (D) control: untreated cells on titanium.

$\times 10^4$  cells were initially seeded per well. Anti-EGFP, a N-terminal primary antibody produced in rabbits,<sup>42,43</sup> was used to compare the levels of EGFP expression. Tubulin was used as the loading control and detected using monoclonal mouse antitubulin antibody.<sup>44</sup>

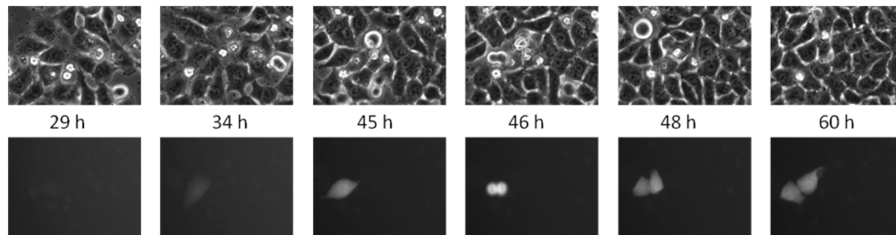


**Figure 5.** Live-cell imaging microscopy of HeLa cells (time-lapse sequences) on CaP/PEI-coated ITO-glass with dripped DNA 29, 34, 45, 46, 48, and 60 h after transfection. Top row: phase contrast microscopy; bottom row: fluorescence microscopy (FITC channel = EGFP fluorescence; magnification 100 $\times$  in all cases).

Confirming to the loading of equal amounts of total protein per well during the SDS-gel running procedure, we found the same amounts of the control protein tubulin by Western blotting in all samples, including the nontransfected negative control. The bands of EGFP were clearly seen in all cases.

The expression of EGFP was different in each case. We clearly observed a strong band in the case of cells transfected with CaP/PEI nanoparticles with later dripped DNA and in the case of CaP/PEI/DNA nanoparticles. After transfection with Polyfect, we also detected an EGFP expression; but in this case the level of expression was lower. These data corroborate the results obtained by flow cytometry and by reflected-light fluorescence microscopy.

In order to determine whether the transfection depended on the cell type, we repeated the experiments with HeLa cells. To monitor the transfection dynamics, we coated ITO glass with nanoparticles and monitored the transfection efficiency by fluorescence microscopy in transmission mode. This was possible because ITO glass is both transparent and electrically conductive. The transfection efficiency was calculated as a ratio of nonfluorescing cells to the total number of cells and is presented in Table 3. The results are in line with the results for NIH3T3 cells reported above.

**Table 3. Efficiency of Gene Transfer in HeLa cells from ITO Substrates as Determined by Fluorescence Microscopy ( $N = 3$ )<sup>a</sup>**

sample	efficiency $\pm$ SD/%
cells on CaP/PEI/DNA nanoparticle coating	3 $\pm$ 4
cells on CaP/PEI nanoparticle coating with dripped DNA	16 $\pm$ 7 ( $P < 0.01$ )
cells on CaP/PEI nanoparticle coating without DNA	0
cells on ITO glass treated with Polyfect as dispersion	13 $\pm$ 8 ( $P < 0.05$ )

<sup>a</sup>P-values are given in comparison to cells cultured on CaP/PEI/DNA coating.

The stability of the transfected EGFP expression level was monitored for 60 h by life-cell imaging. As a typical result, the division of a single cell is shown in Figure 5. The fluorescence intensity of the daughter cells remained on the same level as in the mother cell. Thus, it is likely that both cells contain cEGFP-DNA and still produce EGFP.

## 6. CONCLUSIONS

We developed an easy method of electrophoretic deposition of DNA-loaded calcium phosphate nanoparticles on conducting implants which can be used for an efficient localized gene therapy. The transfection efficiency of such coatings on NIH3T3 cells was comparable to that of commercial reagent

Polyfect and probably achieved due to the locomotion of the cells on the substrate, which led to a better surface contact of the cells with nanoparticles, thereby enhancing the chance of the particles to penetrate the cell membrane. Fluorescent reflected-light microscopy, flow cytometry, and Western Blot showed that cells expressed EGFP after 48 h cultivation on the nanoparticle-coated titanium substrate. Note that the efficiency of transfection from a nanoparticle-coated surface is not easily comparable to a transfection with the same nanoparticles in dispersion. However, the coating of implants with such bioactive nanoparticles helps to avoid the systemic application of gene carriers in nanoparticulate form and therefore to minimize the side effects of such applications.

## AUTHOR INFORMATION

### Notes

The authors declare no competing financial interest.

## ACKNOWLEDGMENTS

We thank the Deutsche Forschungsgemeinschaft (Priority program SPP 1327 to M.E. and H.Z., and general funding to M.E., R.H., and M.K.) for financial support.

## REFERENCES

- (1) Racz, Z.; Hamar, P. Can siRNA technology provide the tools for gene therapy of the future? *Curr. Med. Chem.* **2006**, *13*, 2299–2307.
- (2) Azzam, T.; Domb, A. J. Current development in gene transfection agents. *Curr. Drug Delivery* **2004**, *1*, 165–193.
- (3) Kodama, K.; Katayama, Y.; Shoji, Y.; Nakashima, H. The features and shortcomings for gene delivery of current non-viral carriers. *Curr. Med. Chem.* **2006**, *13*, 2155–2161.
- (4) McNeil, S. E.; Perrie, Y. Gene delivery using cationic liposomes. *Expert Opin. Ther. Pat.* **2006**, *16*, 1371–1382.
- (5) Mello, C. C. Return to the RNAi world: Rethinking gene expression and evolution. *Angew. Chem., Int. Ed.* **2007**, *46*, 6985–94.
- (6) Fire, A. Z. Gene silencing by double-stranded RNA. *Angew. Chem., Int. Ed.* **2007**, *46*, 6966–6984.
- (7) Kurreck, J. RNA Interference: From basic research to therapeutic applications. *Angew. Chem., Int. Ed.* **2009**, *48*, 1378–1398.
- (8) Sokolova, V.; Epple, M. Inorganic nanoparticles as carriers of nucleic acids into cells. *Angew. Chem., Int. Ed.* **2008**, *47*, 1382–1395.
- (9) Berghmans, S.; Jette, C.; Langenau, D.; Hsu, K.; Stewart, R.; Loo, T.; Kanki, J. P. Making waves in cancer research: New models in the zebrafish. *Biotechniques* **2005**, *39*, 227–237.
- (10) Morille, M.; Passirani, C.; Vonarbourg, A.; Clavreul, A.; Benoit, J. P. Progress in developing cationic vectors for non-viral systemic gene therapy against cancer. *Biomaterials* **2008**, *29*, 3477–3496.
- (11) Helm, G. A.; Dayoub, H.; Jane, J. A. Gene-based therapies for the induction of spinal fusion. *Neurosurg. Focus* **2001**, *10*, Article 5.
- (12) Jessel, N.; Oulad-Abdeghani, M.; Meyer, F.; Lavalle, P.; Haikel, Y.; Schaaf, P.; Voegel, J. C. Multiple and time-scheduled in situ DNA delivery mediated by beta-cyclodextrin embedded in a polyelectrolyte multilayer. *Proc. Natl. Acad. Sci. U.S.A.* **2006**, *103*, 8618–8621.

- (13) Jewell, C. A.; Lynn, D. M. Multilayered polyelectrolyte assemblies as platforms for the delivery of DNA and other nucleic acid-based therapeutics. *Adv. Drug Delivery Rev.* **2008**, *60*, 979–999.
- (14) Quick, D. J.; Macdonald, K. K.; Anseth, K. S. Delivering DNA from photocrosslinked, surface eroding polyanhydrides. *J. Controlled Release* **2004**, *97*, 333–343.
- (15) Mei, L.; Jin, X.; Song, C. X.; Wang, M. Y.; Levy, R. J. Immobilization of gene vectors on polyurethane surfaces using a monoclonal antibody for localized gene delivery. *J. Gene Med.* **2006**, *8*, 690–698.
- (16) Jin, X.; Mei, L.; Song, C. X.; Liu, L. X.; Leng, X. G.; Sun, H. F.; Kong, D. L.; Levy, R. J. Immobilization of plasmid DNA on an anti-DNA antibody modified coronary stent for intravascular site-specific gene therapy. *J. Gene Med.* **2008**, *10*, 421–429.
- (17) Itaka, K.; Ohba, S.; Miyata, K.; Kawaguchi, H.; Nakamura, K.; Takato, T.; Chung, U. I.; Kataoka, K. Bone regeneration by regulated in vivo gene transfer using biocompatible polyplex nanomicelles. *Mol. Ther.* **2007**, *15*, 1655–1662.
- (18) Oishi, M.; Hayashi, H.; Itaka, K.; Kataoka, K.; Nagasaki, Y. pH-responsive PEGylated nanogels as targetable and low invasive endosomolytic agents to induce the enhanced transfection efficiency of nonviral gene vectors. *Colloid Polym. Sci.* **2007**, *285*, 1055–1060.
- (19) Meyer, F.; Dimitrova, M.; Jedrzejewska, J.; Arntz, Y.; Schaaf, P.; Frisch, B.; Voegel, J. C.; Ogier, J. Relevance of bi-functionalized polyelectrolyte multilayers for cell transfection. *Biomaterials* **2008**, *29*, 618–624.
- (20) Ren, K. F.; Ji, J.; Shen, J. C. Tunable DNA release from cross-linked ultrathin DNA/PLL multilayered films. *Bioconjugate Chem.* **2006**, *17*, 77–83.
- (21) Lu, Z. Z.; Wu, J.; Sun, T. M.; Ji, J.; Yan, L. F.; Wang, J. Biodegradable polycation and plasmid DNA multilayer film for prolonged gene delivery to mouse osteoblasts. *Biomaterials* **2008**, *29*, 733–741.
- (22) Taori, V. P.; Yemin Liu, Y.; Reineke, T. M. DNA delivery in vitro via surface release from multilayer assemblies with poly-(glycoamidoamine)s. *Acta Biomater.* **2009**, *5*, 925–933.
- (23) Rives, C. B.; des Rieux, A.; Zelyvanskaya, M.; Stock, S. R.; Lowe, W. L.; Shea, L. D. Layered PLG scaffolds for in vivo plasmid delivery. *Biomaterials* **2009**, *30*, 394–401.
- (24) Maitra, A. Calcium-phosphate nanoparticles: Second-generation nonviral vectors in gene therapy. *Expert Rev. Mol. Diagn.* **2005**, *5*, 893–905.
- (25) Pérez-Martínez, F.; Guerra, J.; Posadas, I.; Ceña, V. Barriers to non-viral vector-mediated gene delivery in the nervous system. *Pharm. Res.* **2011**, *28*, 1843–1858.
- (26) Weiner, S.; Wagner, H. D. The material bone: structure-mechanical function relations. *Annu. Rev. Mater. Sci.* **1998**, *28*, 271–298.
- (27) Dorozhkin, S. V.; Epple, M. Biological and medical significance of calcium phosphates. *Angew. Chem., Int. Ed.* **2002**, *41*, 3130–3146.
- (28) Cai, Y.; Tang, R. Calcium phosphate nanoparticles in biominerization and biomaterials. *J. Mater. Chem.* **2008**, *18*, 3775–3787.
- (29) Epple, M.; Ganeshan, K.; Heumann, R.; Klesing, J.; Kovtun, A.; Neumann, S.; Sokolova, V. Application of calcium phosphate nanoparticles in biomedicine. *J. Mater. Chem.* **2010**, *20*, 18–23.
- (30) Hu, J.; Kovtun, A.; Tomaszewski, A.; Singer, B. B.; Seitz, B.; Epple, M.; Steuhl, K. P.; Ergün, S.; Fuchsluger, T. A. A new tool for the transfection of corneal endothelial cells: Calcium phosphate nanoparticles. *Acta Biomater.* **2012**, *8*, 1156–1163.
- (31) Sokolova, V.; Neumann, S.; Kovtun, A.; Chernousova, S.; Heumann, R.; Epple, M. An outer shell of positively charged poly(ethyleneimine) strongly increases the transfection efficiency of calcium phosphate–DNA nanoparticles. *J. Mater. Sci.* **2010**, *45*, 4952–4957.
- (32) Neumann, S.; Kovtun, A.; Dietzel, I. D.; Epple, M.; Heumann, R. The use of size-defined DNA-functionalized calcium phosphate nanoparticles to minimise intracellular calcium disturbance during transfection. *Biomaterials* **2009**, *30*, 6794–6802.
- (33) Sokolova, V.; Kovtun, A.; Prymak, O.; Meyer-Zaika, W.; Kubareva, E. A.; Romanova, E. A.; Oretskaya, T. S.; Heumann, R.; Epple, M. Functionalisation of calcium phosphate nanoparticles by oligonucleotides and their application to gene silencing. *J. Mater. Chem.* **2007**, *17*, 721–727.
- (34) Sokolova, V.; Rotan, O.; Klesing, J.; Nalbant, P.; Buer, J.; Knuschke, T.; Westendorf, A. M.; Epple, M. Calcium phosphate nanoparticles as versatile carrier for small and large molecules across cell membranes. *J. Nanopart. Res.* **2012**, *14*, 910.
- (35) Boccaccini, A. R.; Keim, S.; Ma, R.; Li, Y.; Zhitomirsky, I. Electrophoretic deposition of biomaterials. *J. R. Soc. Interface* **2010**, *7* (Suppl 5), S581–S613.
- (36) Chen, F.; Lam, W. M.; Lin, C. J.; Qiu, G. X.; Wu, Z. H.; Luk, K. D.; Lu, W. W. Biocompatibility of electrophoretical deposition of nanostructured hydroxyapatite coating on roughen titanium surface: In vitro evaluation using mesenchymal stem cells. *J. Biomed. Mater. Res. Appl. Biomater.* **2007**, *82*, 182–191.
- (37) de Sena, L. A.; de Andrade, M. C.; Rossi, A. M.; Soares, G. D. A. Hydroxyapatite deposition by electrophoresis on titanium sheets with different surface finishing. *J. Biomed. Mater. Res. Appl. Biomater.* **2002**, *60*, 1–7.
- (38) Urch, H.; Vallet-Regi, M.; Ruiz, L.; Gonzalez-Calbet, J. M.; Epple, M. Calcium phosphate nanoparticles with adjustable dispersability and crystallinity. *J. Mater. Chem.* **2009**, *19*, 2166–2171.
- (39) Epple, M.; Neumeier, M.; Dörr, D.; LeHarzic, R.; Sauer, D.; Stracke, F.; Zimmermann, H. Electrophoretic deposition of calcium phosphate nanoparticles on a nanostructured silicon surface. *Materialwiss. Werkstofftech.* **2011**, *42*, 50–54.
- (40) Sokolova, V. V.; Radtke, I.; Heumann, R.; Epple, M. Effective transfection of cells with multi-shell calcium phosphate–DNA nanoparticles. *Biomaterials* **2006**, *27*, 3147–3153.
- (41) Urch, H.; Franzka, S.; Dahlhaus, D.; Hartmann, N.; Hasselbrink, E.; Epple, M. Preparation of two-dimensionally patterned layers of functionalised calcium phosphate nanoparticles by laser direct writing. *J. Mater. Chem.* **2006**, *16*, 1798–1802.
- (42) Ormö, M.; Cubitt, A. B.; Kallio, K.; Gross, L. A.; Tsien, R. Y.; Remington, S. J. Crystal structure of the *Aequorea victoria* green fluorescent protein. *Science* **1996**, *273*, 1392–1395.
- (43) Tsukamoto, T.; Hashiguchi, N.; Janicki, S. M.; Tumbar, T.; Belmont, A. S.; Spector, D. L. Visualization of gene activity in living cells. *Nat. Cell Biol.* **2000**, *2*, 871–878.
- (44) Bär, S.; Daeffler, L.; Rommelaere, J.; Nüesch, J. P. F. Vesicular egress of non-enveloped lytic parvoviruses depends on gelsolin functioning. *PLoS Pathog.* **2008**, *4*, e1000126.